Plasma-Surface Reactions at a Spinning Wall

P. F. Kurunczi, J. Guha, and V. M. Donnelly
Department of Chemical Engineering University of Houston, Houston, Texas 77204, USA
(Received 18 July 2005; published 13 January 2006)

We report a new method for studying surface reactions and kinetics at moderately high pressures (<10 Torr) in near real time. A cylindrical substrate in a reactor wall is rotated at up to 200 000 rpm, allowing the surface to be periodically exposed to a reactive environment and then analyzed by a triple-differentially pumped mass spectrometer in as little as 150 μs thereafter. We used this method to study oxygen plasma reactions on anodized aluminum. When the substrate is spun with the plasma on, a large increase in O_2 signal at $m/e = 32$ is observed with increasing rotation frequency, due to O atoms that impinge and stick on the surface when it is in the plasma, and then recombine over the ~0.7 to 40 ms period probed by changing the rotation frequency. Simulations of O_2 signal versus rotation frequency indicate a wide range of recombination rate constants, ascribed to a range of O-binding energies.

DOI: 10.1103/PhysRevLett.96.018306 PACS numbers: 82.33.Xj, 52.40.Hf, 52.77.Bn, 68.43.Mn

Heterogeneous association of atoms and small molecules is an important class of reactions for catalysis [1], combustion [2,3], atmospheric chemistry [4], plasma processing [5–11], and a host of other systems. Most studies of radical-surface reactions fall into one of two categories: beam studies on prepared surfaces in high or ultrahigh vacuum [7,8,12], or stopped-reaction experiments at higher pressures [13,14]. While beam studies at low pressures allow quantitative methods such as line-of-sight mass spectrometry and Auger electron spectroscopy to be used to provide sticking coefficients, product yields, surface coverages, and activation energies, these conditions usually do not simulate very well the processes of interest, where substrates are in a highly reactive and dynamic environment, with very high fluxes of reactants.

One of the best examples is plasma etching of silicon integrated circuits [15,16]. Despite its success, plasma etching is not a well controlled process, due mostly to the complex reactions of neutral radicals and positive ions on the substrate surface and reactor wall [7–11,17]. Small radicals such as Cl, F, O, and CF_2 are formed by electron impact dissociation of feed gases or products. These species react with Al, Si, SiO_2, and polymers to form volatile products such as $AlCl_3$, $SiCl_4$, and CO. Radical densities are determined by the balance between formation and loss reactions. Radicals are lost by formation of etching products, and by wall reactions such as recombination. Larger radicals are also formed by heterogeneous association reactions.

We have begun a new approach to the study of heterogeneous reactions. The method uses a cylindrical substrate coated with the material of choice. The substrate is spun at a rapid rate of up to 200 000 rpm. Therefore, a point on the surface is periodically exposed to the reactants, and then to diagnostic probes in differentially pumped chambers. This allows the surface reactions to be rapidly halted, and products on the surface and desorbing from the surface to be examined as soon as 150 μs thereafter. In this study, we have investigated the recombination of O and desorption of O_2 on anodized Al (a common wall coating in plasma reactors) in an oxygen plasma.

The apparatus consists of an inductively coupled plasma source, an anodized aluminum chamber, the spinning anodized aluminum substrate, and a differentially pumped, line-of-sight mass spectrometer. The reactor wall chamber and cylindrical substrate are depicted in Fig. 1. The substrate motor (Koford, Inc.) can be rotated at up to 200 000 rpm but was not taken above 35 000 rpm in these studies. The 1.27 cm radius spinning substrate is housed in a differentially pumped chamber, with conical skimmers on both sides that follow the contour of the rotating substrate with a constant spacing of ~100 μm. The pressure in this chamber is 1×10^{-5} Torr when the pressure in the plasma chamber is 10 mTorr. The substrate chamber is connected to a differentially pumped intermediate chamber, which is connected to an ultrahigh vacuum chamber that houses a quadruple mass spectrometer (Extrel, 400 amu), and a chopper. Because of the highly oxidizing plasma environment with energetic ion bombardment, the amorphous surface is oxidized and free of carbon or water contaminants.

With the substrate replaced with two aperture plates, line-of-sight mass spectrometry was used to measure an O-atom density (n_0) of 6.8×10^{12} cm^{-3} and a gas temperature of 340 K near the wall at 5 mTorr and 600 W radio-frequency (13.56 MHz) power [18]. Under the same conditions, Langmuir probe measurements at a distance of 0.5–1 cm from the wall yielded a positive ion (overwhelmingly O_2^+ because of the low n_0) density of 8.5×10^9 cm^{-3}, and an electron temperature (T_e) of 5.3 eV [18]. Consequently, the fluxes to the wall (10^{17} cm^2 s^{-1}) were: O_2:O:O_2^+ = 17.6:1.1:0.034.

When the chopper is open, the mass spectrometer signal consists of a line-of-sight beam component of species desorbing from the spinning substrate, a line-of-sight background component from the edges of the skimmer, and an isotropically scattered background gas in the mass spectrometer chamber. With the chopper closed, only the iso-

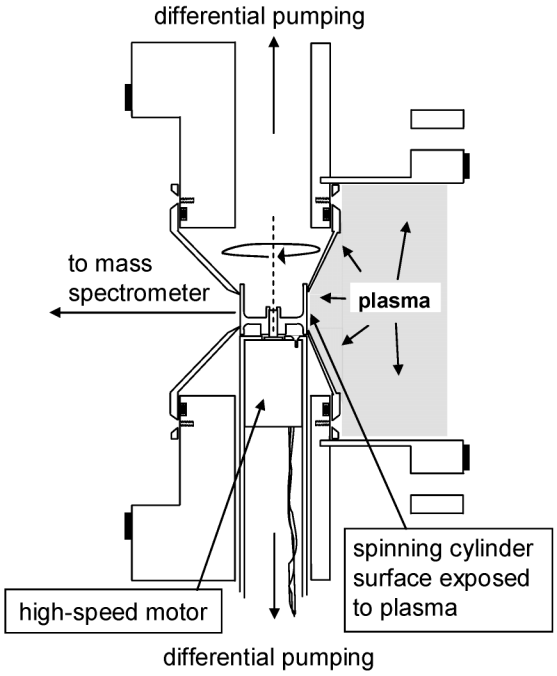

FIG. 1. Side view of the hollow chamber wall containing the rotating cylindrical substrate and conical skimmers.

tropically scattered background gas is detected. Mass spectrometer measurements were recorded as a function of substrate rotation frequency with the plasma off and gas flowing. The measurements were then repeated with the plasma on. Any net increase in signal above the background is due to species that are desorbing from the substrate surface facing the mass spectrometer. At the highest rotation frequencies investigated, this time was 0.7 ms. The temperature of the substrate, measured with a pyrometer, was $30 \pm 5\,^{\circ}\mathrm{C}$. Dual grids in the plasma adjacent to the spinning substrate in some experiments were biased to prevent positive ion bombardment.

A typical set of data is shown in Fig. 2. With O_2 flowing through the chamber and the plasma off, the chopper-open and chopper-closed signals at $m/e = 32$ and 0 rpm are 770 counts and 340 counts, respectively, [Fig. 2(a)], including a background of 130 counts at $m/e = 32$ (with no O_2 in plasma chamber). When the cylinder is rotated, the chopper-open and chopper-closed signals increase by 20%–30% between $r = 0$ and 35 000 rpm, due to additional O_2 that is ''pumped'' from the reactor. The net chopper-open minus chopper-closed signal with the plasma off, S^{off}, is positive because the mass spectrometer detects a line-of-sight flux that leaks around the second skimmer. With the cylinder at rest, the O_2 signals are unchanged when a plasma is ignited [600 W, see left side of Fig. 2(b)]. When the substrate is rotated with the plasma on, however, the signals increase with rotation speed and reach a near-saturation level at $r \approx 30\,000$ rpm [Fig. 2(b)]. Consequently, O_2 is desorbing from the substrate surface over ~0.7 to 30 ms (1/2 a rotation period). Subtracting S^{off} from the chopper-open minus chopper-closed signal with the plasma on (S^{on}) yields D_b^{on}, the net line-of-sight O_2 beam component desorbing from the surface of the cylinder with the plasma on [Fig. 2(c)].

The D_b^{on} signal at $m/e = 32$ is a result of electron impact ionization of O_2 in the mass spectrometer ionizer. No signal is observed with the ionizer off, ruling out the unlikely possibility of O_2^+ desorbing. We also can rule out O_3 (cracking in the ionizer to form O_2^+), since its parent ion is not observed. Plasma negative ions (O^-, O_2^-) cannot reach the substrate due to the repelling plasma sheath potential. We also looked for O desorption. All of the signals at $m/e = 16$ could be attributed to cracking of O_2 in the mass spectrometer ionizer; thus the desorption yield of O is <5% of the O_2 yield.

The only likely explanation for desorption of O_2 is recombination of O atoms. Another possible explanation can be rejected: implantation of O_2^+ leading to neutralization, brief entrainment in the surface, and delayed desorption. Since the ion energy is of the order of $\ln(M_{O2}/m_e)^{1/2}T_e$ [15], (=22 eV) the ''implantation'' depth would be no more than one monolayer; thus a long-lived trapped O_2 seems unlikely. To rule out this mechanism, dual grids were placed in front of the substrate to repel positive ions. Grid #1 (facing the plasma) was biased negatively to repel electrons. Measurements at $m/e = 32$ were carried out at 25 000 rpm with grid #2 grounded or floating to allow positive ions to reach the

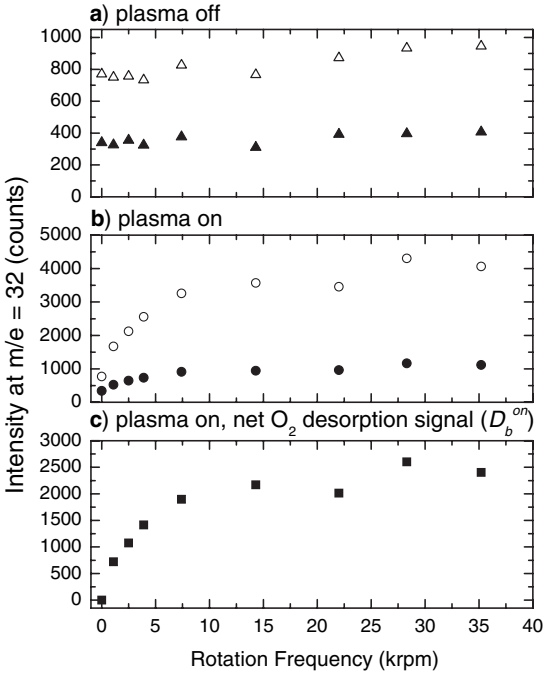

FIG. 2. Chopper-open (open triangles and circles) and chopper-closed (solid triangles and circles) mass spectrometer signals at $m/e = 32$ amu as a function of substrate rotation speed at a pressure of 5 mTorr O_2 for: (a) plasma off, (b) plasma on (600 W), no grids, (c) D_b^{on}, the net O_2 desorption signal.

substrate (collector ion current, $I_i = 145\ \mu$A), or with +100 V bias to block positive ions from reaching the substrate ($I_i = 2\ \mu$A). No significant difference between the O_2 signals is discernible for these two conditions, indicating that positive ions do not contribute significantly to the signals at $m/e = 32$. Also, the relative dependence of the $m/e = 32$ signal on substrate rotation frequency was the same as without the grids, but the signal was half as large, since the 70% open areas of each grid block a total of half the O-atom flux. Hence, O_2^+ and O^+ are not the reactants responsible for formation and desorption of O_2.

At the upper rotation frequency in these experiments (35 000 rpm), the surface velocity ν_S is only 7% of the rms thermal speed of O atoms ($\nu_O = 670$ m/s at 340 K) and therefore makes a negligible distortion of the thermal velocity distribution of the impinging O (the normal incidence angle and speed of O changes by only 4° and 0.2%, respectively). Even at much higher rotation rates than in the present study (e.g., our maximum of 200 000 rpm), ν_S(260 m/s) would add only 50 K to the effective temperature of impinging O.

D_b^{on} measurements for 5 mTorr O_2 plasmas are plotted in Fig. 3 as a function of reaction time, $\Delta t \equiv 1/2r$, the mean time between plasma exposure and observation with the mass spectrometer. The relative decay is larger with higher O flux at 600 W. The time dependencies of product signals in these experiments differ from those in traditional pulsed kinetics methods such as pulsed molecular beam methods in that the method by which Δt is varied affects the starting concentrations at $\Delta t = 0$. This complicates the analysis and interpretation of decay curves.

To illustrate this, consider a too-simple model for the current experiment in which O atoms adsorb at vacant sites by a Langmuir-Hinshelwood process, and recombine in a second-order reaction with a coverage-independent rate constant, k_r.

$$O_{(g)} + S \rightarrow O_{(ads)} \quad (1)$$

$$2O_{(ads)} \xrightarrow{k_r} O_{2(g)} + 2S, \quad (2)$$

where S is a site for O adsorption and the $O_{(ads)}$ binding energy is high enough that O desorption is unimportant. Weakly bound O_2 immediately desorbs and reaction (2) can be considered as a single step. The amount of $O_{2(g)}$ desorbing from the surface is given by $d[O_{2(g)}] = k_r[O_{ads}]^2 dt$. $[O_{(ads)}]_t$, the coverage of $O_{(ads)}$ at a time t after an initial time t_i, when the $O_{(ads)}$ coverage is $[O_{(ads)}]_i$, is given in integrated form by $[O_{(ads)}]_t = \frac{(\sqrt{a}-b)\exp(C_i)+\sqrt{a}+b}{2k_r[\exp(C_i)-1]}$, with $C_i = \sqrt{a}(t-t_i) + \ln(\frac{b+\sqrt{a}+2k_r[O_{(ads)}]_i}{b-\sqrt{a}+2k_r[O_{(ads)}]_i})$, $a = sf(4k_r + \frac{sf}{[S]_0^2})$, and $b = sf/[S]_0$, with s being the sticking coefficient at a vacant site, f the O flux to the surface when it is in the plasma, and $[S]_0$ the total number of sites.

A point on the substrate surface midsection is periodically in the plasma, and then removed from the plasma. Time, t, is $(n + \theta/2\pi)/r$, where n is the number of complete cycles and θ is the phase angle. $\theta = 0$ when the point on the surface is centered in the plasma, and π when it faces the mass spectrometer. The point is in the plasma and the O-atom flux is f for $-\phi < \theta < \phi$ and out of the plasma ($f = 0$) for $\phi < \theta < 2\pi$-ϕ, where $\phi = 63°$.

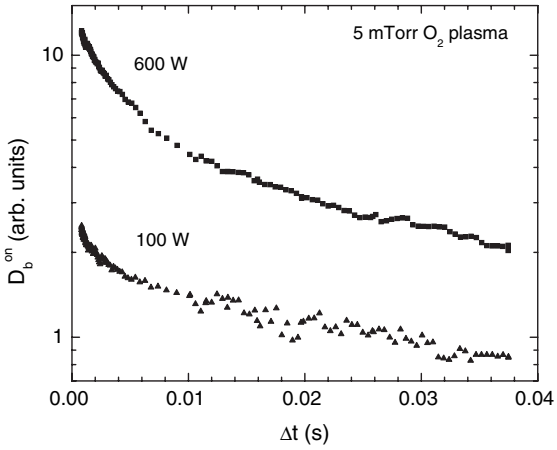

FIG. 3. D_b^{on} for O_2 vs reaction time (reciprocal of twice the rotation frequency) for a 5 mTorr O_2 plasma, at 600 and 100 W of plasma power. No grids were present between the sample and the plasma.

To simulate the measurements, $[O_{(ads)}]_t$ must be evaluated at the beginning and end of each plasma exposure period until a periodic steady state is reached. $[O_{(ads)}]_t$ was computed for the simple second-order recombination mechanism above. When the rate of O-atom recombination is slow relative to the rotation speed (e.g., at 80 000 rpm with $k_r = 1 \times 10^{-13}$ cm^2 s^{-1}, $s = 1$, $[S]_0 = 1 \times 10^{15}$ cm^{-2}, $f = 1 \times 10^{17}$ cm^{-2} s^{-1}), the depth of modulation in $[O_{(ads)}]_t$ is small (1%) and the approach to steady state requires many cycles (~ 60). Conversely, when the recombination rate is fast compared to the rotation rate (at 1000 rpm), the depth of modulation is large (70%) and steady state is reached in only 2 cycles.

Steady-state O_2 desorption signals computed at $\theta = \pi$ as a function of Δt are plotted in Fig. 4 for a 10^5-fold variation in the O recombination rate constant. For very small values of k_r, the desorption rate is much slower than the rotation rate, and the signal is nearly independent of reaction time to the longest available time (0.04 s). Under this limiting condition, the signal increases nearly linearly with k_r. As k_r is increased beyond $\sim 10^{-13}$ cm^2 s^{-1}, the signal at longer reaction times (e.g., 0.04 s) reaches a maximum and then decreases. This decrease occurs when the reaction time is faster than the rotation time.

The simulations can be compared with the measurements in Fig. 3. Observed O_2 signals decay by a factor of 3 to 6 between 0 and 0.04 s, depending on discharge power. The simulation predicts a similar (fourfold) decay for $k_r = 1 \times 10^{-12}$ cm^2 s^{-1}. The shape of this simulated decay is very different than the observed decays, however, predicting a small rise between 0 and 0.005 s. The observed signals decay more rapid initially (0–0.01 s) and more

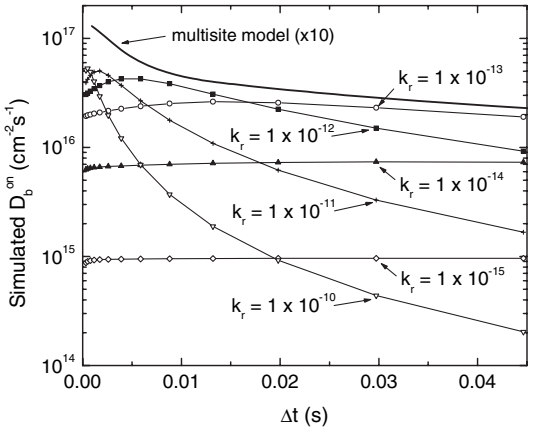

FIG. 4. Simulations of D_b^{on} vs reaction time (reciprocal of twice the rotation frequency) at $\theta = \pi$. Lines with symbols: simple second-order recombination mechanism, $s = 1$, $f = 1 \times 10^{17}$ cm^2 s^{-1}, $[S]_0 = 1 \times 10^{15}$ cm^{-2}. Thick line without symbols: multisite model [18] (multiplied by 10 before plotting).

slowly at longer times. Shapes similar to the measurements are predicted for larger k_r ($\sim 10^{-10}$ cm^2 s^{-1}), but with much larger falloffs ($\sim$200-fold) than observed over 0.04 s. No combination of f, $[S]_0$, and k_r in this simple mechanism can reproduce the observations.

To capture the shape and magnitude of the measured decays we need to invoke a mechanism with a very large decrease in recombination rates as a function of increasing time and decreasing O coverage (i.e., effective recombination rate constants of 10^{-10} cm^2 s^{-1} at early times, decreasing to 10^{-13} cm^{-2} s^{-1} at longer times). We have achieved this (Fig. 4, ''multisite model'') with a mechanism in which O atoms reversibly adsorb at and desorb from sites with a distribution of binding energies. The model is similar to that of Cartry *et al.* [19] and Kim and Boudart [20] for O recombination on silica, in that mobile O diffuses from site to site and recombines or desorbs. The model also produces a recombination coefficient for O on oxygen-plasma-exposed anodized Al of 0.6. A detailed discussion of this model is beyond the scope of this Letter and will be reported elsewhere [18].

In summary, a new, rotating substrate method is reported for studying surface reactions in reactive, moderately high pressures (<10 Torr from extrapolations) environments. The technique has been used to gain new insights into O-atom surface recombination on anodized aluminum surfaces immersed in an oxygen plasma. This new approach to studying surface reactions should have many added applications in plasma processes, catalysis, combustion, and atmospheric chemistry such as reaction of radicals on particles and ice crystals.

This work was supported by the American Chemical Society's Petroleum Research Fund (Grant No. 39922-AC5S) and equipment donations from Agere Systems and Bell Laboratories, Lucent Technologies. V. M. D. acknowledges a conversation circa 1995, in which a collaborator, Keith Guinn, suggested a similar idea of spinning a flat silicon wafer between a plasma etching reactor and an analysis chamber.

[1] P. Granger, P. Malfoy, P. Esteves, L. Leclercq, and G. Leclercq, Catalysis **187**, 321 (1999).
[2] A. N. Hayhurst and A. D. Lawrence, Prog. Energy Combust. Sci. **18**, 529 (1992).
[3] G. Loffler, D. Andahazy, C. Wartha, F. Winter, and H. Hofbauer, J. Ener. Resources Tech.-Trans. of the ASME **123**, 228 (2001).
[4] S. Seisel, B. Fluckiger, F. Caloz, and M. J. Rossi, Phys. Chem. Chem. Phys. **1**, 2257 (1999).
[5] I. P. Herman, V. M. Donnelly, K. V. Guinn, and C. C. Cheng, Phys. Rev. Lett. **72**, 2801 (1994).
[6] C. C. Cheng, K. V. Guinn, V. M. Donnelly, and I. P. Herman, J. Vac. Sci. Technol. A **12**, 2630 (1994).
[7] E. R. Fisher, Plasma Sources Sci. Technol. **11**, A105 (2002).
[8] G. P. Kota, J. W. Coburn, and D. B. Graves, J. Vac. Sci. Technol. A **16**, 270 (1998).
[9] G. Cunge, R. L. Inglebert, O. Joubert, L. Vallier, and N. Sadeghi, J. Vac. Sci. Technol. B **20**, 2137 (2002).
[10] G. Cunge, M. Kogelschatz, and N. Sadeghi, Plasma Sources Sci. Technol. **13**, 522 (2004).
[11] G. Cunge, M. Kogelschatz, and N. Sadeghi, J. Appl. Phys. **96**, 4578 (2004).
[12] H. C. Flaum, D. J. D. Sullivan, and A. C. Kummel, J. Phys. Chem. **98**, 1719 (1994).
[13] R. M. Robertson and M. J. Rossi, J. Chem. Phys. **91**, 5037 (1989).
[14] W. Muller-Markgraf, M. J. Rossi, J. Phys. Chem. **95**, 825 (1991).
[15] M. A. Lieberman and A. J. Lichtenberg, *Principles of Plasma Discharges and Materials Processing* (Wiley, New York, 1994).
[16] *Plasma Etching: An Introduction*, edited by D. M. Manos and D. L. Flamm (Academic, New York, 1989).
[17] A. R. Godfrey, S. J. Ullal, L. B. Braly, E. A. Edelberg, V. Vahedi, and E. S. Aydi, Rev. Sci. Instrum. **72**, 3260 (2001).
[18] P. F. Kurunczi and J. Guha, V. M. Donnelly, J. Phys. Chem. B **109**, 20 989 (2005).
[19] G. Cartry, L. Magne, and G. Cernogora, J. Phys. D **33**, 1303 (2000).
[20] Y. C. Kim and M. Boudart, Langmuir **7**, 2999 (1991).